

Does Bulk Metallic Glass of Elemental Zr and Ti Exist?

Takanori Hattori, Hiroyuki Saitoh, Hiroshi Kaneko, Yuka Okajima, Katsutoshi Aoki, and Wataru Utsumi

Synchrotron Radiation Research Center, Japan Atomic Energy Agency, Kouto 1-1-1, Sayo-cho, Sayo-gun, Hyogo 679-5148, Japan

(Received 8 March 2006; published 30 June 2006)

To verify the high-pressure formation of the bulk metallic glass in elemental Zr and Ti, which Zhang and Zhao [Nature (London) **430**, 332 (2004)] and Y. Wang *et al.* [Phys. Rev. Lett. **95**, 155501 (2005)] recently reported, the high-pressure states were investigated by our newly developed *in situ* angle-dispersive x-ray diffraction using a two-dimensional detector and x-ray transparent anvils. Despite the disappearance of all the Bragg peaks in the one-dimensional energy-dispersive data, two-dimensional angle-dispersive data showed several intense Bragg spots even at the conditions where the amorphization was reported. This finding suggests that Zr and Ti do not transform into an amorphous state, but that their grain size becomes large, which causes the missing Bragg peaks in energy-dispersive data.

DOI: [10.1103/PhysRevLett.96.255504](https://doi.org/10.1103/PhysRevLett.96.255504)

PACS numbers: 81.05.Kf, 07.35.+k, 61.10.Eq

Bulk metallic glasses exhibit excellent mechanical properties because of aperiodic atomic arrangements and the resulting nonexistence of dislocations and crystal plane gliding. These have been produced by rapidly cooling the melts at a sufficient rate to suppress crystallization [1]. In the early 1990s, new glass-forming compounds with very small critical cooling rates, less than 100 K/s, were discovered in zirconium-based systems [2]. Thus, cm-sized metallic glass can be merely obtained by typecasting the melts into copper molds and this novel class of materials is being used for engineering applications.

For the formation of the bulk metallic glass, multicomponent systems, which consist of several elements with a significant size mismatch, are practically indispensable to frustrate the crystallization on cooling [1]. In contrast, pure elemental Zr was recently reported to transform into an amorphous state at high pressures and at temperatures much lower than its melting point [3]. Then, another group IV element, Ti, was also reported to show an almost identical behavior [4]. These are significant matter because both glasses are one-component systems and as such are unlikely to show phase separation at high temperatures, which is different from typical multicomponent metallic glasses. Actually, these glasses appear to have high-thermal stability [stable up to at least 1000 °C [3,4]].

In the both elements, the amorphization was reported to occur through the following process [3,4]. First, the ambient α phase (hcp structure) transformed into the high-pressure ω phase (distorted hcp structure) by room-temperature compression. As the temperature was elevated into the stable region of the high-temperature β phase (bcc), the pattern changed into that of the β phase [5] and, after a short period, all the Bragg peaks vanished as if it had transformed into an amorphous state. Upon cooling to ambient temperature, the amorphouslike pattern remained in Zr, but it reverted to that of a crystalline phase in Ti. Based on the disappearance of all the Bragg peaks, previous studies concluded that these materials had amorphized. Since these behaviors were more clearly observed near their α - ω - β triplet points, this phe-

nomenon was interpreted in terms of the phase confusion model [4].

Although clear results were shown in the previous works, their data have several points that are inconsistent with amorphization: (i) on the *absolute* scale (or on the scale with a fixed exposure time) the baseline of the x-ray profiles did not significantly increase after amorphization, which is inconsistent with the general feature that the height of the diffuse maxima in an amorphous state is typically about one-tenth of that of the highest peak in the crystalline state. (ii) Despite the high-thermal stability, the amorphous Ti reverted to its crystalline phase upon cooling [4]. The high-thermal stability indicates that the glass transition temperature T_g is much higher than 1000 °C. Thus, the recrystallization is unlikely to occur during cooling. These observations imply that something other than amorphization occurred under high *PT* condition.

The ambiguity of the high-pressure state of Zr and Ti originates from insufficient information on the state of matter, which is often encountered in high-pressure experiments. One of the most serious problems is in the method used to detect the diffracted x rays. In the previous experiments, the energy-dispersive x-ray diffraction (EDX) method, which is a standard technique for high-pressure experiments using a multianvil press, was employed. However, this technique provides limited information, namely, the diffracted x rays that pass through the gap between the high-pressure anvils. This occasionally leads to the misinterpretation of the state of matter when the Debye rings are not uniform. Observations of a two-dimensional image of the diffracted x rays are indispensable to overcome this problem. In addition to the EDX method, this study used a recently developed angle-dispersive x-ray diffraction (ADX) method, which employs a two-dimensional detector in conjunction with a multianvil press equipped with x-ray transparent anvils [6]. Despite the disappearance of all the Bragg peaks in the EDX data, the ADX data showed very intense Bragg spots from Zr and Ti even under the high-*PT* conditions where amorphization was reported. This finding suggests

that Zr and Ti maintain their crystalline forms under high- PT conditions and that the disappearance of all the Bragg peaks in the EDX data originates from missing the Bragg spots in the measuring window due to rapid grain growth. This rapid grain growth occurs at relatively low temperatures (less than half the melting point). Although this phenomenon is unexpected because typically this low temperature does not induce grain growth, this phenomenon is explained by the anomalous lattice dynamics and the resulting anomalous fast self-diffusion in β -Zr and -Ti.

Experiments were performed by *in situ* x-ray diffraction using a multianvil high-pressure apparatus, SMAP180, installed in the beam line BL14B1 at SPring-8 [7]. Both the ADX and EDX methods were employed to reveal the high-pressure states of Zr and Ti more accurately. Here, we briefly compare both methods to show the advantages of the ADX method (Fig. 1). The EDX system consists of six tungsten-carbide anvils and a solid-state detector (SSD). The diffraction data are collected through the narrow gap between the anvils (typical width is 0.3 mm). This system acquires data only from a limited area in a two-dimensional diffraction pattern. Therefore, this system occasionally leads to the misinterpretation when the Debye rings are not uniform. On the other hand, our ADX system consists of x-ray transparent anvils made of cubic boron nitride [6] and a two-dimensional imaging plate detector (IP). The diffracted x rays that pass through the anvils are collected by IP over a wide solid angle. Therefore, this system provides more reliable information on the state of matter even when the Debye rings are not uniform. This is significant especially under high-pressure and high-temperature conditions where materials often crystallize into large grains.

The high-pressure states of Ti and Zr were investigated along the pressure and temperature path where amorphization was previously reported. Since the impurity in the sample often affects the high- PT behavior [8], we used the same ultrahigh purity Zr that Zhang and Zhao [3] used in their studies. For Ti, we used a commercially available sample, which was 99.9% pure (Nilaco Co. Ltd.). A sample, which had a 1.0 mm diameter and was 0.6 mm high, was placed in a hexagonal boron-nitride capsule. The

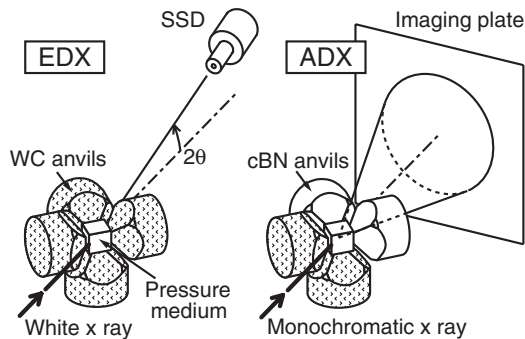


FIG. 1. Schematic view of the experimental setup in the angle- and energy-dispersive x-ray diffraction methods.

capsule was set in a graphite tube furnace and was encased in a pressure-transmitting medium made of a mixture of boron and epoxy resin. The temperature was monitored with a WRe5%–WRe26% thermocouple. The pressure was calculated based on the equation of state for a NaCl pressure marker [9]. In the ADX experiments, we used a monochromatic x-ray beam (60 keV), which was collimated to 0.3 mm \times 0.3 mm.

The EDX method was initially employed to confirm the previous results of Zhang and Zhao [3] and Wang *et al.* [4]. Our EDX data were identical to their results (Fig. 2). For Zr, the α phase began to transform into the ω phase near 4 GPa and the single ω phase was obtained at 7.7 GPa by room-temperature compression. Upon increasing the temperature to 600 °C, the phase remained. However, further increasing the temperature to 650 °C caused the sharp diffraction peaks to rapidly vanish and only weak humps were observed as if it had transformed to an amorphous state. The Ti sample showed an almost identical behavior (The amorphouslike pattern was observed over wide pressure region between 2.0 and 10.4 GPa.)

In contrast to the EDX data, the ADX data showed a completely different behavior. Figures 3(a)–3(c) show typical x-ray diffraction images of Zr. Complete Debye rings from the ω phase were observed at 8.3 GPa and 500 °C (additional rings from the boron pressure-medium and the boron-nitride sample capsule were also present) [Fig. 3(a)]. The phase transition to the β phase began at 650 °C. The diffraction pattern appeared not as entire

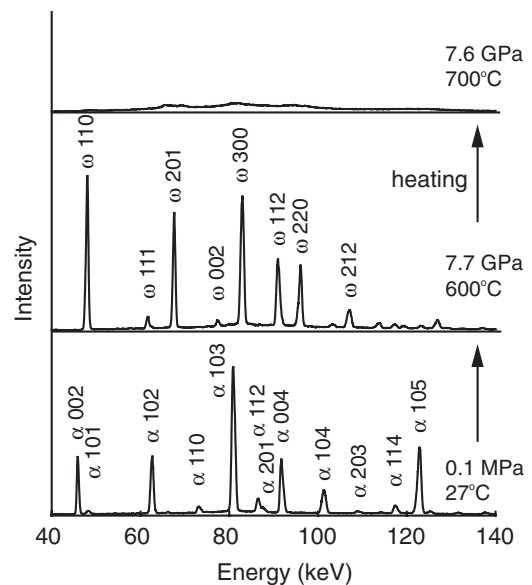


FIG. 2. X-ray diffraction profiles of Zr at high pressures and high temperatures obtained in an energy-dispersive mode. Starting material (α phase) transformed into the ω phase near 4 GPa. Then all the Bragg peaks disappeared at 7.7 GPa and 650 °C as if it had transformed into an amorphous state. The profiles were collected for an exposure time of 100 sec. It is noteworthy that the intensity of the baseline is maintained while heating from 600 °C to 700 °C.

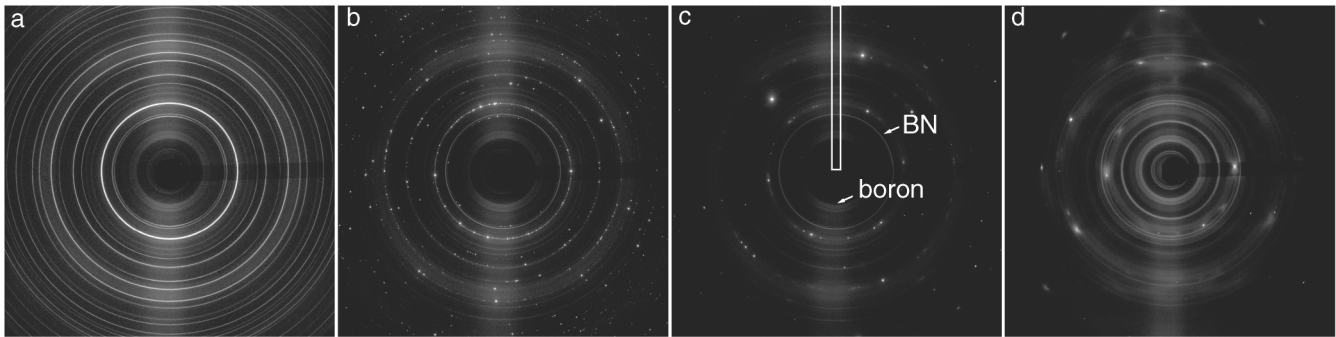


FIG. 3. X-ray diffraction images of Zr and Ti at high pressures and high temperatures obtained in an angle-dispersive mode. (a) Complete Debye rings from the ω -Zr at 8.3 GPa and 500 °C. (b) Phase transition to the β -Zr begins at 8.3 GPa and 650 °C. (c) Bragg spots from the β -Zr at 8.1 GPa and 700 °C. Debye rings are from boron and hexagonal boron nitride. The strip along the vertical axis represents the region where the diffraction data is obtained in the energy-dispersive measurement. (d) X-ray diffraction image of Ti at 10.7 GPa and 1050 °C. Debye rings are from boron and hexagonal boron nitride.

rings, but as numerous small Bragg spots along the rings [Fig. 3(b)]. When the temperature was further increased to 700 °C, only a few strong Bragg spots were observed [Fig. 3(c)]. This diffraction image indicates that grains aggregated and formed several single crystals, which are comparable to or even larger than the incident x-ray beam size (0.3 mm \times 0.3 mm). The strong Bragg spots were maintained upon further increasing the temperature to 1000 °C. While heating, a one-dimensional profile, $I(2\theta)$, converted from the diffraction image did not show a significant increase in its baseline, which is expected if amorphization had occurred. Thus, the ADX data do not provide evidence for amorphization. These results were reproduced in all the experimental runs that we conducted. The same behavior was also observed in Ti. As the temperature increased at $P = 10.8$ GPa, the Debye ring from the ω phase became spotty and upon further increasing the temperature, only several intense Bragg spots were observed in the β -phase stable region (additional rings are from the boron pressure-medium and the boron-nitride sample capsule) [Fig. 3(d)]. After cooling to room temperature, numerous Bragg spots from the ω or α phase, depending on the pressure range, appeared. These results suggest that Zr and Ti maintained their crystalline forms even at high- PT conditions, even though the EDX data showed the amorphouslike pattern. These experimental results were also confirmed by another ADX experiment using a multichannel collimator [10] installed in the beam line BL22XU at SPring-8, which allows a diffraction image to be almost completely obtained from the sample. Here, a mixing state of amorphous and crystalline forms in both Zr and Ti was ruled out since the rapid grain growth by fast atomic movements and amorphization due to freezing of atomic movements would not take place coincidentally.

The apparent inconsistency between the EDX and ADX data is explained as follows. The EDX experiment uses a large volume press, which limits the diffracted x-ray measurements through the small gap between the anvils. The

measurement corresponds to a scan in the narrow strip shown in Fig. 3(c). When the grains grow under high- PT conditions, the Bragg spots are likely outside of the measuring window. Thus, diffracted x rays from the sample may be missed, which is exactly what we observed in the EDX experiments on Zr and Ti. In contrast, our ADX method measures the diffracted x rays over wide cubic angle through x-ray transparent anvils. Considering the rapid grain growth, the strange features of the EDX data can be explained. (i) The much lower baseline than expected for the amorphous state is due to its nonexistence, and (ii) the apparent back-transformation from the amorphous state into the crystalline state, which Wang *et al.* [4] reported in Ti, is due to the transformation from the β phase with large grain size into the low-temperature phases with small grain size.

Although the disappearance of all the Bragg peaks in the EDX data is explainable by the rapid grain growth of Zr and Ti, the rapid grain growth in the low-temperature range (less than half of the melting point) is *a priori* strange because generally the atoms are insufficiently mobile to form large grains at such low temperatures. However, the rapid grain growth is possible with the help of the anomalous lattice dynamics and the resulting anomalous fast self-diffusion, which are both well-known properties in bcc Zr and Ti [11–14]. It is known that all elements in groups 3, 4, 5, and 6 commonly have a bcc structure and that the bcc structure becomes less stable in the order from group 6 to group 3. In this family, group 4 elements (Ti, Zr, Hf) have anomalous phonon dispersion; the longitudinal phonon branch is very soft at the wave vector $\mathbf{q} = \frac{2}{3}(111)$ (the energy transfer is almost zero) [11–13]. Hence, the amplitude of the lattice vibration is quite large. The self-diffusion is enhanced by this large lattice vibration and becomes anomalously fast [14]. Since these are only characteristic of the bcc structure, the crystal would rapidly grow as the sample is heated into the β -phase stable region. In addition, the preservation of the crystallographic orientation during the transition should enhance the grain

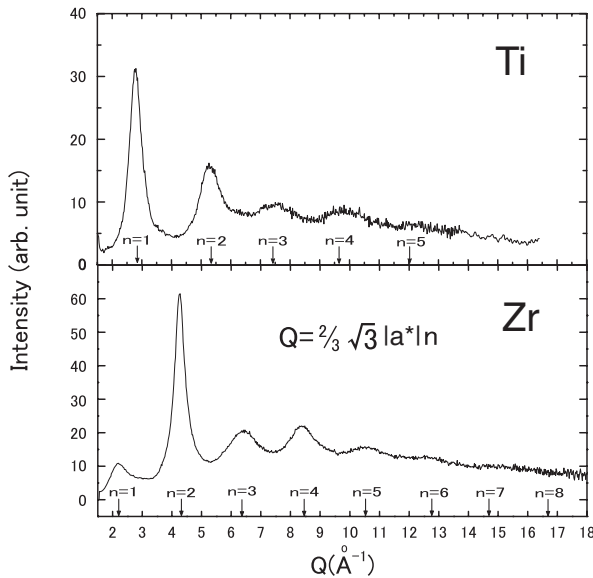


FIG. 4. Diffuse scattering intensity of bcc Zr at 7.5 GPa and 1000 °C and that of bcc Ti at 10.4 GPa and 1000 °C. Arrows on the abscissa show Q positions that correspond to $\frac{2}{3}\sqrt{3}|a^*| \times n$ (n is an integer).

growth. The low-temperature phases (α and ω) transform into the β phase while maintaining the following crystallographic relations [12,15,16]:

$$(110)_{\beta} \parallel (0001)_{\alpha} \quad \text{and} \quad [\bar{1}11]_{\beta} \parallel [\bar{2}110]_{\alpha}$$

$$(111)_{\beta} \parallel (0001)_{\omega} \quad \text{and} \quad [\bar{1}11]_{\beta} \parallel [0110]_{\omega}.$$

In this case, six α -phase variants (four ω -phase variants) can merge into a single domain of the β phase. For these reasons, the grains become large even at relatively low temperatures.

Although the hump observed in the EDX data is too low to be explained by amorphous formation, it is larger than the typical baseline for crystalline phases [Actually, this confused the state of Zr and Ti in the previous studies [3,4].] To reveal its nature, we analyzed the amorphouslike pattern and compared these patterns to those previously reported in diffuse scattering studies [17,18]. In the past, two-dimensional scattering intensity has been collected by x-ray and neutron scattering to reveal the lattice dynamics near the β - α transition in Zr [18] and near the β - ω transition in $Zr_{1-x}Nb_x$ alloys [17]. The results showed that the relatively strong diffuse scattering, which is related to the intrinsic lattice instability of the β phase toward the α or ω phase, appeared at scattering vector $\mathbf{Q} = \frac{2}{3}(111) \times n$ (n is an integer) [cf. Fig. 5 in Ref. [17], Fig. 9 in Ref. [18], and Fig. 4 in Ref. [19]]. Figure 4 is our result on the Q dependence of the scattering intensity of bcc Zr and bcc Ti [20]. The humps are located at scattering vector $Q = \frac{2}{3} \times \sqrt{3}|a^*| \times n$ (n is an integer), which are consistent with the results of the previous scattering studies. Therefore, the anomalously large baseline observed in Zr and Ti is attrib-

uted to the diffuse scattering, which is related to the lattice instability in the β phase.

The present study using a newly developed ADX method belies the amorphous formation of elemental Zr and Ti, which has been claimed from EDX experiments [3,4]. The EDX method is a standard and established technique for high- PT experiments using a large volume press, which is common at most major synchrotron facilities. The present study provides instructive caution; energy-dispersive data must be carefully analyzed to correctly interpret the state of matter, especially in noncrystalline materials research.

The authors thank J. Zhang and Y. Zhao for supporting the experiments and Yanbin Wang for his technical advice. We are also grateful to M. Hasegawa for his useful discussions.

- [1] J.F. Löffler, *Intermetallics* **11**, 529 (2003).
- [2] A. Inoue, *Acta Mater.* **48**, 279 (2000).
- [3] J. Zhang and Y. Zhao *Nature (London)* **430**, 332 (2004).
- [4] Y. Wang *et al.*, *Phys. Rev. Lett.* **95**, 155501 (2005).
- [5] The detailed phase relation of α -, ω -, and β -Ti is shown in Ref. [21].
- [6] Y. Wang, W. B. Durham, I. C. Getting, and D. J. Weidner, *Rev. Sci. Instrum.* **74**, 3002 (2003).
- [7] W. Utsumi *et al.*, *J. Phys. Condens. Matter* **14**, 10497 (2002).
- [8] R. G. Henning *et al.*, *Nat. Mater.* **4**, 129 (2005).
- [9] D. L. Decker, *J. Appl. Phys.* **42**, 3239 (1971).
- [10] K. Yaoita *et al.*, *Rev. Sci. Instrum.* **68**, 2106 (1997).
- [11] C. Stassis, J. Zarestky, and N. Wakabayashi, *Phys. Rev. Lett.* **41**, 1726 (1978).
- [12] W. Petry *et al.*, *Phys. Rev. B* **43**, 10933 (1991).
- [13] A. Heiming *et al.*, *Phys. Rev. B* **43**, 10948 (1991).
- [14] W. Petry *et al.*, *Phys. Rev. Lett.* **61**, 722 (1988).
- [15] U. Pinsook and G. J. Ackland, *Phys. Rev. B* **58**, 11252 (1998).
- [16] H. R. Wenk, I. Lonardelli, and D. Williams, *Acta Mater.* **52**, 1899 (2004).
- [17] W. Lin, H. Spalt, and B. W. Batterman, *Phys. Rev. B* **13**, 5158 (1976).
- [18] O. Dubos, W. Petry, J. Neuhaus, and B. Hennion, *Eur. Phys. J. B* **3**, 447 (1998).
- [19] J. R. Morris and K. M. Ho, *Phys. Rev. B* **63**, 224116 (2001).
- [20] The data were collected by the EDX method, which allowed the diffuse scattering intensity to be almost completely obtained from the sample. To obtain the scattering intensity over wide Q region, the data were collected at several detector angles. A detailed procedure to connect these data and remove the distortion of the intensity profile, which originates from the energy dependence of the detection efficiency of the SSD, is shown in Refs. [22,23].
- [21] S. Pecker *et al.*, *J. Appl. Phys.* **98**, 043516 (2005).
- [22] T. Hattori *et al.*, *Phys. Rev. B* **68**, 224106 (2003).
- [23] K. Tsuji *et al.*, *Rev. Sci. Instrum.* **60**, 2425 (1989).